Isocitrate Dehydrogenase from *Azotobacter vinelandii*. Order of Substrate Addition and Product Release†

Jeffrey S. Wicken,‡ Albert E. Chung, and James S. Franzen*

ABSTRACT: The TPN-specific isocitrate dehydrogenase from *Azotobacter vinelandii* has been subjected to steady state kinetics analysis. The kinetics of the uninhibited reaction and product inhibition patterns indicate that the forward direction substrates add in a rapid equilibrium random manner and that the products are released predominantly in the order of CO_2, 2-ketoglutarate, and TPNH. The system is complicated, under appropriate conditions, by the formation of two dead-end complexes, one of the enzyme with isocitrate and TPNH, and the other with TPN^+ and 2-ketoglutarate. Directly determined dissociation constants are reported for all the expected binary enzyme–substrate complexes, the active ternary complex, E–TPNH–KG, and the dead-end complexes. The carboxylate group of D-isocitrate which is lost during the reaction is shown to depart as molecular CO_2 rather than as the HCO_3^- anion. The character of the pH dependency of the Michaelis constant for molecular CO_2 gives support to the notion that CO_2 is not covaletly bound, say, as a carbamate, but is held by secondary valence forces.

The TPN[1]-specific isocitrate dehydrogenase from *Azotobacter vinelandii* has been shown to be a monomeric enzyme having a molar mass of 80,000 daltons and containing three sulfhydryl groups of varying reactivity (Chung and Franzen, 1969). It catalyzes the transfer of hydrogen from the substrate, *threo*-D_s-isocitrate, with A type TPN specificity and the decarboxylation of the substrate with retention of configuration (Chung and Franzen, 1970). The most reactive sulfhydryl group is not directly involved in the catalytic process, since it can be quantitatively converted to a thiocyanate group with the resulting derivatized enzyme possessing about 40% of the native specific activity (Chung *et al.*, 1971). The order of substrate addition in the reverse direction of TPNH first, followed successively by 2-ketoglutarate and either HCO_3^- or CO_2, has been implicated (Chung and Franzen, 1970).

Thompson and Cleland have carried out product inhibition studies on the TPN-specific isocitrate dehydrogenase from pig heart and have concluded that a mechanism involving random substrate addition and ordered product release in the sequence of CO_2, 2-ketoglutarate, and TPNH was likely (Thompson and Cleland, 1965). Colman and Chu have reported that isocitrate and 2-ketoglutarate bind to this pig heart enzyme with respective dissociation constants of 2.25 and 4.62 μM (Colman and Chu, 1970). Using a fluorescence technique, Langan determined the dissociation constants for the binary complex of TPNH and TPN^- with TPN-specific isocitrate dehydrogenase from pig heart homogenates to be on the order of 0.01 and 2.0 μM, respectively (Langan, 1960). Since the dissociation constant for the complex of enzyme and 2-ketoglutarate is about 500 times as large as that for the TPNH complex, it is not unlikely that the major amount of 2-ketoglutarate generated during the enzymatic reaction is released prior to TPNH. Also, the nearly identical dissociation constants of the binary complexes formed by the enzyme with TPN and isocitrate support the suggestion of Thompson and Cleland regarding the random addition of substrate. Londesborough and Dalziel have proposed a similar scheme for the reaction catalyzed by the TPN-linked isocitrate dehydrogenase from beef heart mitochondria (Londesborough and Dalziel, 1970). Their kinetic data, however, favor a significant contribution from an alternative pattern of product release, *viz.* CO_2, TPNH, and 2-ketoglutarate.

This study was undertaken as part of an overall effort to understand the mechanistic details of the *Azotobacter* enzyme and the molecular bases from which the catalytic similarities, or differences, of the various isocitrate dehydrogenases derive. Evidence is herein provided pertaining to the order of substrate addition in both the forward and reverse directions, the identity of the decarboxylation product as molecular CO_2, the mode of association of CO_2 with the enzyme, and the existence of certain dead-end complexes.

Experimental Section

Materials. The substrates and cofactors for the enzyme were purchased from Sigma. Radiolabeled materials such as 2-ketoglutarate-^{14}C and sodium DL-isocitrate-5,6-^{14}C, 0.1 Ci mol^{-1}, were procured from the Amersham-Searle and the New England Nuclear Corp., respectively. Other chemicals were obtained as reagent grade products from commercial suppliers. Isocitrate dehydrogenase was prepared essentially according to the earlier described procedure, yielding a specific activity of about 130 standard enzyme units per milligram (Chung and Franzen, 1969). The preparation procedure was modified from this earlier reported method by the omission of the carboxymethylcellulose fractionation and by the addition of a second pass through Sephadex G-100 of the concentrated enzyme obtained by the reported method.

Determination of Kinetic Constants. The progress of enzymatically catalyzed reactions was monitored by recording the

† From the Department of Biochemistry of the Faculty of Arts and Sciences, University of Pittsburgh, Pittsburgh, Pennsylvania 15213. *Received July 17, 1972.* Supported in part by grants from the National Institutes of Health (AM12104 and AM14290).

‡ Supported by a National Science Foundation predoctoral stipend. This material was submitted in partial fulfillment of the Ph.D. degree in biochemistry at the University of Pittsburgh (1971). Present address: Department of Chemistry, Arizona State University, Tempe, Ariz.

[1] Abbreviations used are: TPN, triphosphopyridine nucleotide; TPNH, reduced triphosphopyridine nucleotide; KG, 2-ketoglutarate; IC, isocitrate; ORD, optical rotary dispersion; CD, circular dichroism.

absorbance at 340 nm of rapidly mixed solutions using a Cary 14R recording spectrophotometer equipped with a 0.0–0.1 slide-wire. Initial velocities were evaluated from the slopes of the progress curves within the first 10 sec of the reaction. Reactions were initiated by the addition of 5, 10, or 15 μl of enzyme solution to a cuvet maintained at 25°, which generally contained a total of 2.0 ml of 0.05 M potassium phosphate buffer (pH 7.3), 0.005 M $MgCl_2$, and determined quantities of substrates, cofactors, and inhibitors as subsequently specified. Exceptions to this practice will be explicitly indicated. All solutions were prepared from glass redistilled water. The concentrations of stock substrate solutions of isocitrate and TPN^+ were determined using limiting amounts of one substrate with an excess of the other in the presence of the enzyme and employing the change in 340-nm absorbance to compute the desired concentration. Since 2-ketoglutarate could not reliably be completely converted to isocitrate by excess TPNH and CO_2, concentrations of stock solutions of this substrate were determined by the glutamic dehydrogenase method (Williamson and Corkey, 1969).

Primary plots of reciprocal initial velocity *vs.* reciprocal substrate concentration were based on duplicate velocity measurements at each variable substrate concentration. The slopes and intercepts of the primary plots were obtained by the weighted linear least-squares method outlined by Cleland (1967). Similarly, slopes and intercepts of secondary (or tertiary) replots were obtained by the weighted linear least-squares technique, the weighting of data points being inversely proportional to the variance in the dependent variable, *i.e.*, to the variance in the corresponding primary (or secondary) plot slope or intercept. For the forward reaction, the kinetic constants of interest were obtained from secondary plots of the type just mentioned, while for the reverse reaction the Michaelis constants for each of the three substrates were evaluated directly from primary plots obtained with saturating levels of the two substrates other than the one under consideration. To obtain the compound kinetic constants characteristic of the reverse reaction, however, third-order replots were required which necessitated the use of a $4 \times 4 \times 4$ matrix of substrate concentrations. Hence, TPNH and $NaHCO_3$ concentrations were varied independently over ranges appropriate to their Michaelis constants at each of the four levels of 2-ketoglutarate employed. For accurate values of apparent bicarbonate concentrations ($HCO_3^- + CO_2$) to be obtained in these reaction mixtures, it was necessary to use buffers containing insignificant amounts of CO_2 predissolved from the atmosphere. This was accomplished by freshly preparing buffers from glass distilled water that had been boiled and stored under ascarite.

V_{max}–pH Profile. Rate measurements in the forward direction, oxidative decarboxylation, were made in the presence of 1×10^{-4} M TPN^+, 4×10^{-3} M DL-isocitrate, and 5×10^{-3} M magnesium chloride at 25°. Potassium phosphate, Tris-HCl, and glycine–KOH, all at 0.05 M with respect to total buffer species, were the selected buffers for the pH ranges of 5.0–7.2, 7.2–8.5, and 8.5–11.0, respectively. The degree of independence of rate with respect to buffer type was assessed by overlapping the buffer ranges as indicated. No special precautions were taken, in the case of V_{max} measurements, to maintain constant ionic strength throughout the pH range covered. Unless there were fortuitous mutual cancellations of ionic strength and buffer effects at the above two overlapping pH values, the omission of specific measures to maintain constant ionic strength was justified. To separate possible denaturation effects from the activity profile, the enzyme was incubated for various prolonged times in the buffer of interest and then added to the standard assay medium at pH 7.0 and 30° for the determination of its specific activity. Though prolonged exposure to the low and high pH limits employed resulted in irreversible activity losses, such losses were negligible over the period, less than 20 sec, required for the assays here in question.

Rate measurements of the reverse reaction, reductive carboxylation, were made at 25° in the presence of 1×10^{-4} M TPNH, 2×10^{-2} M 2-ketoglutarate, and 5×10^{-3} M magnesium chloride at two high but nonsaturating levels of sodium bicarbonate, 3.2×10^{-2} M and 6.4×10^{-2} M. Potassium phosphate buffer was used through pH 7.4 and Tris-HCl buffer was used from pH 7.8 to 8.5, both at concentrations of only 0.025 M. Because of practical difficulties in working at actual saturating concentrations of apparent total bicarbonate over the pH range studied, the values of the reciprocal velocities at the two bicarbonate concentrations employed were extrapolated to zero reciprocal bicarbonate concentration in order to obtain V_{max} for the reverse reaction.

CO_2 vs. HCO_3^- as the Carboxylation Substrate. The method of Dalziel and Londesborough was employed to differentiate between the two possible forms of the carboxylation substrate that might be released from the enzyme–TPNH–oxalosuccinate complex (Dalziel and Londesborough, 1968). For studies using bicarbonate as the initiating species, reaction mixtures were prepared containing 8×10^{-5} M TPNH, 1×10^{-2} M 2-ketoglutarate, 5×10^{-3} M $MgCl_2$, and an appropriate amount of enzyme in 1.8 ml of 0.1 M potassium phosphate buffer. To avoid contamination by carbon dioxide dissolved from the atmosphere, all solutions were freshly prepared from distilled water that had been boiled and then stored under Ascarite. The reactions were initiated by the addition of 0.2-ml portions of unbuffered 0.01 M Na_2CO_3 solution to the above reaction mixtures which were maintained at 17°, and the reaction was followed by measurement of the decay of absorbance at 340 nm. The change in pH with time following the addition of Na_2CO_3 was measured on similar samples. To determine whether the magnitude of this pH change, never greater than 0.05 unit, significantly affected the disposition of the progress curves, initial velocity measurements were made on reaction mixtures containing preequilibrated 1×10^{-3} M HCO_3^-–CO_2 solutions at pH values that spanned the observed pH change range. It was observed that the rate changes due to the pH increase resulting from the spontaneous conversion of HCO_3^- to CO_2 were from 5 to 10% depending on the range of the initial pH. Such a rate change was insignificant compared to that occurring in nonequilibrated solutions.

For studies using CO_2 as the initiating species, a saturated solution of CO_2 in water was prepared by bubbling CO_2 from Dry Ice sublimation into about 20 ml of water maintained at 17° for 1 hr prior to use. At 17° the solubility of total CO_2 in water is 0.04 M (Dalziel and Londesborough, 1968). The reactions were initiated by the addition of 0.2 ml of this CO_2 solution to reaction solutions containing TPNH, 2-ketoglutarate, and $MgCl_2$ as described just above, and buffered to either pH 6.4 or 7.1 with 0.1 M potassium phosphate or to pH 8.0 with 0.1 M Tris-HCl. As before, the reactions were run at 17°. For comparison, initial velocities were also measured in systems containing 4×10^{-3} M preequilibrated HCO_3^-–CO_2 at pH values corresponding to those above. Again, the rate change due to the slight pH drop was insignificant relative to that observed in nonequilibrated solutions.

Ultrafiltration Binding Measurements. Binding ratios were

ascertained by the use of an Amicon Model 8-MC microultrafiltration unit operated in either the concentration or diafiltration mode, depending on the design of the experiment as will be described. Differential filtration was accomplished with the PM-30 type membrane (Amicon) under a pressure of 10 psi.

The binding isotherm of TPN^+ was obtained by operation in diafiltration mode as follows. The enzyme solution, about 1.5 ml at an enzyme concentration of about 4 mg/ml, was placed in the ultrafiltration chamber, and about 20 ml of the corresponding TPN^+ solution was placed in the reservoir. The effluent solution was assayed for TPN^+ by measuring the change in A_{340} following the addition of enzyme and excess isocitrate. After diafiltration, sufficient to bring the ligand concentration of the filtrate to that of the reservoir, 5–8 ml, the enzyme solution was removed as quantitatively as possible from the ultrafiltration chamber and weighed in a tarred container on an analytical balance. From the initial enzyme concentration and volume and the final gravimetrically determined volume, the final enzyme concentration could be evaluated. The TPN^+ concentration was determined in the enzyme solution by the A_{340} change produced by added excess isocitrate. To assure that an insignificant loss of enzyme activity occurred during diafiltration, the enzyme solution before and after diafiltration was assayed according to the standard procedure described above. Data were considered reliable for binding ratio calculations if initial and final activities disagreed by less than 5%.

The same general procedure was followed for the binding of D-isocitrate; however, isocitrate was assayed by scintillation counting of ^{14}C-labeled DL-isocitrate. A dioxane based scintillation fluid was employed containing 5 g of 2,5-diphenyloxazole and 100 g of naphthalene per liter of solution. Enzyme concentrations in the ultrafiltration chamber were measured by 280-nm absorption in this case (Chung and Franzen, 1969). It was assumed that L-isocitrate did not bind to the enzyme in these experiments. The agreement between the binding data derived from ultrafiltration and differential optical rotary dispersion (ORD) methods (described below) and the inactivity of L-isocitrate as a substrate support the reasonableness of this assumption.

For the binding of TPNH, the filtrate TPNH concentration was obtained by direct 340-nm absorbance measurement. The measurement of bound TPNH in the enzyme containing solution in the ultrafiltration chamber required a correction for the different 340-nm extinction coefficients of bound and free TPNH (Chung and Franzen, 1970), and for a slight contribution by protein absorbance. Protein concentration, in the presence of ligand at the end of diafiltration, was determined by gravimetric volume measurement and the measurement of enzymatic activity in a medium containing 0.025 M phosphate at pH 7.3, 5×10^{-3} M $MgCl_2$, 1×10^{-2} M 2-ketoglutarate, 5×10^{-3} M $NaHCO_3$, and about 6×10^{-5} M TPNH in a total volume of 2.0 ml. Agreement of specific activities between initial and final enzyme solutions within 5% was the criterion for data retention.

The binding of 2-ketoglutarate was determined by the same general procedure as that used in the isocitrate experiments. A stock ligand solution was made by dissolving the commercial sample of freeze-dried 2-ketoglutarate-^{14}C in a solution of unlabeled 2-ketoglutarate. The final concentration of 2-ketoglutarate in the stock solution was determined by glutamic dehydrogenase assay (Williamson and Corkey, 1969). Because 2-ketoglutarate bound less tightly to the enzyme than did other substrates studied, it was necessary to use higher enzyme concentrations, approximately 6 mg/ml.

The formation of the ternary enzyme–substrate complex, E–TPNH–KG, and the ternary dead-end complexes, E–TPNH–IC and $E–TPN^+–KG$, was studied by measuring the binding of one of the ligands in the presence of saturating, or nearly saturating, quantities of the other ligand. In experiments involving the complex, E–TPNH–KG, the enzyme was diluted from stock with a solution prepared from carbon dioxide free buffer and high concentrations of either TPNH or 2-ketoglutarate, depending on the choice of variable ligand. An appropriate amount of the other ligand was then added to this solution, which was then placed in the ultrafiltration chamber. To minimize the dissolution of CO_2 introduced from the atmosphere during assembly, the unit was operated in concentration mode. The concentration of free ligand does not change as the solution is concentrated, so that the concentration of ligand in the effluent could be assumed to represent the concentration of free ligand in equilibrium with bound ligand. Only one data point was obtainable from a given solution, because of uncertainties accumulating over more extended times due to the slow reaction occurring with the small amounts of dissolved CO_2.

The dead-end complexes, E–TPNH–IC and $E–TPN^+–KG$, were also studied in this manner, with the exception that the binding of TPN^+ to the enzyme in the presence of 2-ketoglutarate was not attempted because the technique used to measure TPN^+ required the absence of KG in the reaction mixture. The general unfeasibility of making accurate enzymic assays on solutions involved in these determinations limited the data yield of each solution to one point on the saturation curve. In all cases of ternary complex formation the enzyme concentration at the conclusion of the experiment was determined employing gravimetric volume measurement.

ORD–CD Binding Measurements. Rotation and ellipticity measurements were performed on the Cary-6001 spectropolarimeter at ambient temperature. The technique of differential ORD measurements for the determination of complex formation between isocitrate and the enzyme and between isocitrate and Mg^{2+} ion was carried out according to the directions of Adkins and Yang (Adkins and Yang, 1968). In the case of the formation of the enzyme–substrate complex wherein it is presupposed that the enzyme binds only one of the enantiomorphic forms of DL-isocitrate, the method becomes especially simple. To the reference cell, containing enzyme, only volumes of buffer, equivalent to the volumes of buffered DL-isocitrate added to the sample cell, need be added. As is evident from eq 1–4, if the molar rotation of the enzyme–substrate complex is different from the sum of the molar rotations of the free enzyme and the free substrate, an amount of rotation will be observed which is proportional to the concentration of complex.

$$\alpha_{\lambda,\text{obsd}} = \alpha_{\lambda,\text{sample}} - \alpha_{\lambda,\text{ref}} \tag{1}$$

$$\alpha_{\lambda,\text{sample}} = \frac{d}{100}\{[\phi]_E(c_E^0 - c_{ES}) + [\phi]_D(c_D^0 - nc_{ES}) + [\phi]_L c_L^0 + [\phi]_{ES} c_{ES}\} \tag{2}$$

$$\alpha_{\lambda,\text{ref}} = \frac{d}{100}[\phi]_E c_E^0 \tag{3}$$

Since $[\phi]_C = -[\phi]_D$ and $c_L^0 = c_D^0$

$$\alpha_{\lambda,\text{obsd}} = \frac{d}{100}\{[\phi]_{ES} - ([\phi]_E + n[\phi]_D)\}c_{ES} \tag{4}$$

TABLE I: Initial Velocity Parameters for the Oxidative Decarboxylation and Reductive Carboxylation Reactions Catalyzed by Isocitrate Dehydrogenase.[a]

Oxidative Decarboxylation[b]	Reductive Carboxylation[c]
$V_f/E = 8.0 \times 10^3$ min^{-1}	$V_r/E = 5.8 \times 10^3$ min^{-1}
$K_{TPN^+} = (2.0 \pm 0.7) \times 10^{-5}$ M	$K_{TPNH} = (9.2 \pm 5.4) \times 10^{-6}$ M
$K_{IC} = (1.7 \pm 0.6) \times 10^{-5}$ M	$K_{KG} = (1.4 \pm 0.8) \times 10^{-3}$ M
$K'_{TPN^+} = (2.0 \pm 0.9) \times 10^{-5}$ M	$K_{HCO_3^-(t)} = (8.5 \pm 0.1) \times 10^{-3}$ M
$K'_{IC} = (1.8 \pm 0.8) \times 10^{-5}$ M	$K_{TPNH,KG} = (2.8 \pm 0.8) \times 10^{-8}$ M
	$K_{TPNH,CO_2} = (1.9 \pm 3.3) \times 10^{-8}$ M^2
	$K_{KG,CO_2} = (1.2 \pm 0.2) \times 10^{-5}$ M^2
	$K_{TPNH,KG,CO_2} = (2.9 \pm 0.5) \times 10^{-10}$ M^3

[a] The Michaelis constant for total (HCO_3^- + CO_2), $K_{HCO_3^-(t)}$, was determined at pH 7.1 and at 17°. All the other parameters were determined at pH 7.2 and 26°. [b] Determined in 0.05 M potassium phosphate buffer. [c] Determined in 0.025 M potassium phosphate buffer.

In the above expressions, α, $[\phi]$, and c represent rotations in degrees, molar rotations, and molar concentrations, respectively. The path, d, is expressed in centimeters. The substrate D-isocitrate is added to the sample cell at concentration c_D^0 as half of the racemic pair.

ORD studies were also performed to assess the stability of the Mg^{2+}–isocitrate chelate. The rotation changes at a fixed wavelength produced by the addition of $MgSO_4$ to a cell containing the natural substrate *threo*-D_s-isocitrate were used to calculate the amount of chelate formed. The mechanical zero of the instrument was adjusted so that the cell containing substrate initially caused a midscale positioning of the recording pen.

Results

Initial Velocity Patterns. The primary double reciprocal plots for either substrate of the forward reaction as the variable substrate at different fixed levels of the other substrate were linear and showed a common point of intersection on the negative abscissa. Though these data by themselves reveal nothing about the order of substrate addition, they demonstrate that a ternary complex of the enzyme and both isocitrate and TPN^+ is formed prior to the release of any of the reaction products. For the reverse reaction, the double reciprocal plots for each substrate with virtually saturating quantities of the remaining two substrates were linear. The mechanisms of the forward and reverse reactions must therefore obey the general rate equation, eq 1 (Dalziel, 1969). For the

$$\frac{1}{v} = \frac{1}{V}\left(1 + \frac{K_a}{A} + \frac{K_b}{B} + \frac{K_c}{C} + \frac{K_{ab}}{AB} + \frac{K_{bc}}{BC} + \frac{K_{ac}}{AC} + \frac{K_{abc}}{ABC}\right) \quad (5)$$

forward reaction any terms in C are omitted. The variables A, B, and C represent substrate concentrations, and the K values are the various Michaelis and compound constants. The presence or absence of certain terms of the general rate equation will have mechanistic significance. The values of the various kinetic parameters yielded by initial velocity studies are shown for both the forward and reverse reactions in Table I. The constants K'_{TPN^+} and K'_{IC} of Table I are the slope to intercept ratios of the appropriate secondary replots. The value of the compound constant $K_{TPN^-,IC}$ is obtained as the product of either K'_{TPN^+} and K_{IC}, or of K'_{IC} and K_{TPN}. All of the forward reaction kinetic constants were easily measured and were internally consistent. For the reverse reaction, only the individual Michaelis constants and the compound constants, K_{KG,CO_2} and K_{TPNH,KG,CO_2} had sufficient magnitude to be readily measured. The compound constants $K_{TPNH,KG}$ and K_{TPNH,CO_2}, on the other hand, were both small and of doubtful significance. Figure 1 illustrates the dependency of the reverse reaction velocity on either TPNH or apparent HCO_3^- concentrations at saturating levels of 2-ketoglutarate. The form of these velocity–substrate functions has special relevance to the question of the order of substrate addition in the reverse direction as is elaborated in the Discussion.

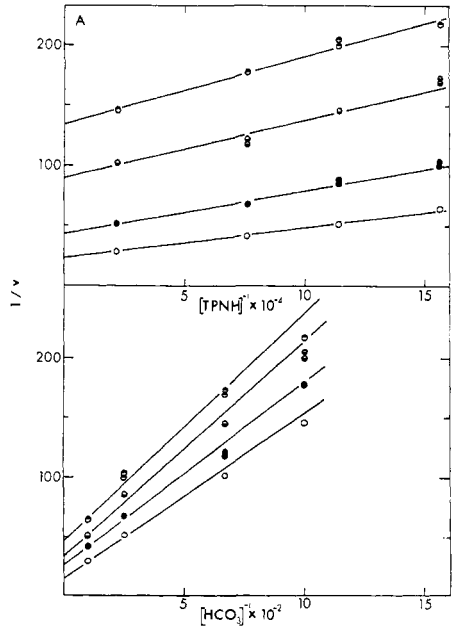

FIGURE 1: Primary double reciprocal reverse reaction plots at an essentially saturating concentration, 0.04 M, of 2-ketoglutarate. (A) TPNH as variable substrate; HCO_3^- as fixed substrate at molar concentrations × 10^3 of: 10.0 (○); 4.0 (●); 1.5 (◒); 1.0 (◓). (B) HCO_3^- as variable substrate; TPNH as fixed substrate at molar concentrations × 10^5 of: 4.55 (○); 1.32 (●); 0.88 (◒); 0.64 (◓).

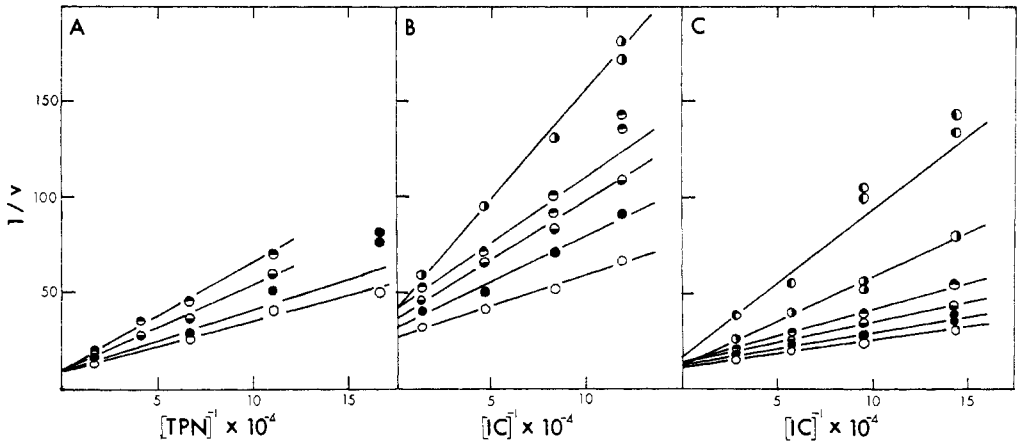

FIGURE 2: Primary double reciprocal plots of the forward reaction with TPNH as a product inhibitor. (A) TPN as variable substrate; D-isocitrate as fixed substrate at 5×10^{-5} M concentration. [TPNH] $\times 10^5$: 0.0 (○); 2.5 (●); 5.0 (◒); 7.5 (◓). (B) D-Isocitrate as variable substrate under standard assay conditions; TPN^+ as fixed substrate at 1.1×10^{-5} M. [TPNH] $\times 10^5$: 0.0 (○); 2.1 (●); 4.2 (◒); 6.3 (◓); 8.4 (◑). (C) D-Isocitrate as variable substrate in 0.05 M Tris–0.02 M $MgCl_2$ buffer, pH 8.3; TPN^+ as fixed substrate at 5.6×10^{-5} M. [TPNH] $\times 10^5$: 0.0 (○); 0.44 (●); 1.1 (◒); 3.8 (◓); 5.6 (◑); 7.0 (◐).

Product Inhibition Relations. Figure 2 shows the product inhibition patterns for the forward reaction with TPNH as the product inhibitor. TPNH behaves as a competitive inhibitor against TPN^+ at all concentrations of fixed substrate (isocitrate) tested, Figure 2A. The magnitude of the inhibition by a product, P, is customarily described in terms of inhibition constants, $K_{i,P}$, which are defined in terms of slope or intercept effects. The ratio of the slope (or intercept) in the presence of inhibitor to the slope (or intercept) in the absence of inhibitor can be expressed as $1 + [P]/K_{i,P}^{slope}$ (or $1 + [P]/K_{i,P}^{int}$). According to this formulation, inhibition vanishes as the inhibition constant increases in magnitude without limit. The inhibition constants for the competitive inhibition of TPNH against TPN^+ under the conditions corresponding to Figure 2A are plotted in Figure 3A against the various concentrations of fixed substrate (isocitrate) studied. The salient feature of Figure 3A is that $K_{i,TPNH}^{slope}$ does not increase linearly with isocitrate concentration as would be expected for an uncomplicated competitive inhibition in which TPN^+ and TPNH simply compete for the same site on the free enzyme.

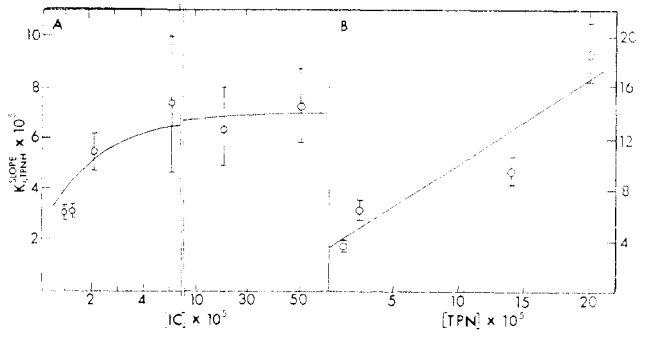

FIGURE 3: The dependence of TPNH product inhibition constants on the concentration of fixed substrate for the forward reaction. (A) The variation of $K_{i,TPNH}^{slope}$ as determined by the effect of TPNH on the slope of $1/v$ *vs.* 1/[TPN] plots, with the concentration of D-isocitrate present in the reaction system. (B) The variation of $K_{i,TPNH}^{slope}$ as determined by the effect of TPNH on the slope of $1/v$ *vs.* 1/[IC] plots, with the concentration of TPN^+ present in the reaction system.

The initial rise in $K_{i,TPNH}^{slope}$ with increasing isocitrate levels and the attainment of a limiting value of $K_{i,TPNH}^{slope}$ at high isocitrate levels are consistent with the postulation of the formation of a dead-end complex; see Discussion.

Against isocitrate, inhibition by TPNH is noncompetitive under the assay conditions employed but the intercept variation is not large; Figure 2B. The slope TPNH inhibition constants corresponding to a series of experiments of the type illustrated in Figure 2B at varying levels of fixed substrate, TPN^+, bear a linear dependency on the concentration of TPN^+, Figure 3B. The intercept TPNH inhibition constants appropriate to these experiments had such great individual variability that it was not possible to determine reliably what sort of dependency they had on the level of fixed substrate, TPN^+.

For reasons developed later, it was thought that the postulated dead-end complex formation could be eliminated at higher pH and Mg^{2+} ion concentrations and that in such a situation TPNH would exhibit competitive inhibition against isocitrate as the variable substrate. This was accomplished by using higher levels of $MgCl_2$ (0.02 M) than in previous experiments and by replacing phosphate buffer at pH 7.3 with Tris buffer (chloride anion) at pH 8.3. Under these conditions, TPNH acts as a competitive inhibitor of isocitrate, Figure 2C.

2-Ketoglutarate served as the other product inhibitor of the forward reaction behaving uncompetitively with respect to TPN^+ as variable substrate and noncompetitively with respect to isocitrate as variable substrate.

In the reverse reaction, both TPN^+ and isocitrate were found to be competitive inhibitors of TPNH as the variable substrate. Against 2-ketoglutarate as the variable substrate, the inhibition by TPN^+ was noncompetitive, whereas the inhibition by isocitrate while noncompetitive showed only a very small intercept effect.

pH Effects on Kinetic Parameters. The pH dependency of the turnover numbers of *A. vinelandii* isocitrate dehydrogenase for both the forward and reverse reactions was essentially Gaussian. For the forward reaction a maximum turnover number of 15,000 min^{-1} was obtained at pH 8.5. Half-maximum velocity occurred at pH values of 7.2 and 9.8. The reverse reaction velocity was greatest at pH 8.0, where the turnover number was 7500 min^{-1}. Half-maximum velocity oc-

TABLE II: Michaelis Constants for TPN^+, Isocitrate, TPNH, and 2-Ketoglutarate at Various pH Values.

pH	K_{TPN^+}[a,b]	K_{IC}[a,b]	K_{TPNH}[a,c]	K_{KG}[a,c]
6.5	4.0 ± 1.2	2.0 ± 2.7	6.3 ± 0.4	13.7 ± 1.3
6.7			6.3 ± 0.3	12.6 ± 9.0
7.0	7.6 ± 3.6	7.6 ± 0.5		
7.2	8.3 ± 9.8	6.8 ± 5.4	9.2 ± 5.4	13.9 ± 8.2
7.5	5.2 ± 1.5	4.6 ± 4.1	6.4 ± 0.6	11.5 ± 0.4
8.0	8.0 ± 0.3	3.2 ± 0.7		
8.2			10.7 ± 0.7	19.8 ± 1.3
8.5	10.3 ± 0.9	7.8 ± 0.9		
9.4	7.5 ± 0.3	10.5 ± 0.7		

[a] The values are all expressed as M × 10^6. [b] Phosphate buffer was used for pH values 6.5, 7.0, and 7.2 with the ionic strength being maintained at 0.053. Tris-HCl buffer was used at pH values 7.5, 8.0, and 8.5 and glycine-KOH at pH 9.4. The ionic strengths at these latter pH values were 0.053, 0.008, 0.029, and 0.044, respectively. [c] Phosphate buffer, 0.025 M, was used from pH 6.5 through pH 7.2. Tris buffer, 0.025 M, was used at higher pH values.

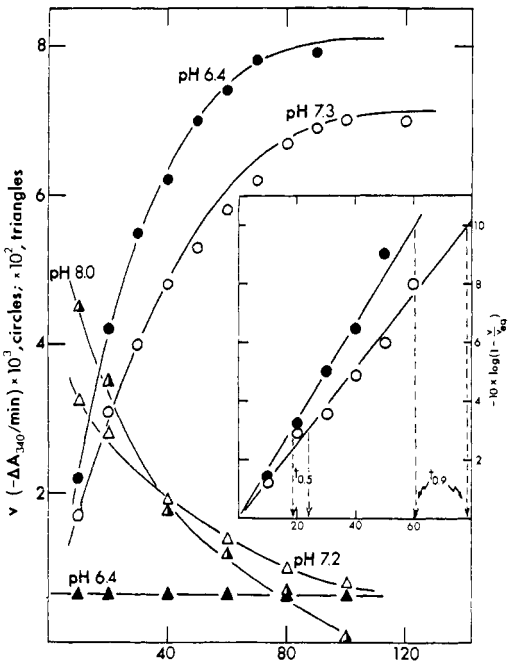

FIGURE 4: Reductive carboxylation reaction velocity variation with time after the addition of sodium carbonate or carbon dioxide.

curred at pH 6.8 on the acid side. A complete rate–pH profile was not obtained for the reverse reaction because of the difficulty in obtaining saturation by CO_2 at high pH values.

The values of the kinetic constants for the forward reaction obtained from secondary replots of initial velocities at various values of pH are listed in Table II. Note that care was exercised to maintain a constant ionic strength of 0.053 from pH 6.5 to 7.5. It is evident that these constants bear little or no pH dependency. Under conditions where no precautions were taken to control the ionic strength, apparent variations of the kinetic constants with pH were observed, but the variations were irregular with changes in pH and only on the order of fourfold in magnitude at most. It could be argued that such apparent variability could have arisen from specific ion effects superimposed on ionic strength effects; however, the data of Table II collected from experiments performed in three different buffer systems give no support to this contention. The Michaelis constants for TPNH and 2-ketoglutarate obtained from the reductive carboxylation reaction are also listed in Table II as a function of pH. A constant buffer concentration of 0.025 M was used in all these determinations with no special effort being made to control ionic strength. Again, little or no pH dependency of these constants is indicated.

CO_2 vs. HCO_3^- as the Carboxylation Substrate. The velocities of the reductive carboxylation reaction at pH 6.4 and 7.2, initiated by the addition of unbuffered sodium carbonate solutions, are graphed as functions of time in Figure 4. The inset of Figure 4 portrays the plots of $-\log(1 - (v/v_{eq}))$ *vs.* time for the carboxylation reaction at these two pH values, along with an indication of the times at which the velocities reach 0.5 and 0.9 of their respective limiting values. The rate *vs.* time curves obtained for reactions at pH 6.4, 7.2, and 8.0 initiated by the addition of unbuffered CO_2 solutions are also shown in Figure 4. Significant amounts of the preequilibrium CO_2 were consumed in this reaction relative to the amounts of CO_2 remaining at or near equilibrium in the absence of reductive carboxylation. Hence, the data cannot be legitimately plotted in the logarithmic form which relates enzymatic reaction velocities to the rate constant for the spontaneous decay of CO_2 to bicarbonate.

In Table III, the initial velocities obtained for the reductive carboxylation at different pH values using CO_2 as the initiating form are compared with the corresponding initial velocities for reactions using preequilibrated HCO_3^-–CO_2 solutions at an overall concentration of 4×10^{-3} M. Notice that with increasing pH, the ratio of velocities in the unbuffered and preequilibrated reaction mixtures increases as does the ratio of CO_2 concentrations in the unbuffered and buffered reaction mixtures. In the former mixture the initial ratio of CO_2 to HCO_3^- is constant though of uncertain magnitude.

The Michaelis constants for total HCO_3^- ($HCO_3^- + CO_2$), $K_{HCO_3^-(t)}$, and for CO_2 only, K_{CO_2}, are given at various pH levels in Table IV. The latter constants were obtained by multiplying the values of $K_{HCO_3^-(t)}$ by the term $(1 + 10^{pH-6.35})^{-1}$ where the quantity 6.35 represents the negative logarithm of the equilibrium constant for the reaction $CO_2 + H_2O \rightleftharpoons HCO_3^- + H^+$ (Harned and Owen, 1958). In the region of maximum catalytic activity occurring between pH values 7.4 and 8.4, these constants exhibit the general behavior with respect to pH that is expected for a system wherein CO_2, rather than HCO_3^-, is the true substrate, *i.e.*, K_{CO_2} remains approximately constant throughout this pH range, whereas $K_{HCO_3^-(t)}$ increases, reflecting the progressively diminishing CO_2–$HCO_3^-(t)$ ratios. In contrast to the Michaelis constants obtained for the other substrates of this enzyme, K_{CO_2} is a sensitive function of pH below 7.4. The implications of this variation are treated in the Discussion.

Mg^{2+} Ion Effects. Since the overall oxidative decarboxylation reaction has a requirement for Mg^{2+} ions (Chung and Franzen, 1969), the kinetic parameters describing the reaction were evaluated at different Mg^{2+} ion concentrations and are set forth in Table V. It is evident that, among these parameters, only the Michaelis constant for isocitrate is significantly affected by changing the concentration of $MgCl_2$. This sort of behavior was also observed with the beef heart enzyme

TABLE III: Comparison of Initial Velocities Obtained with Reaction Mixtures Utilizing Preequilibrated HCO_3^-–CO_2 Solutions and Those Utilizing Unbuffered CO_2 Solutions.

	Preequilibrated			Unbuffered		$V_{unbuffered}$
pH	HCO_3^-[a]	CO_2[a]	v_{PE}[b]	CO_{2total}[a]	v_U[b]	V_{preeq}
6.4	2.0	2.0	5.4	4.0	6.0	1.1
7.1	3.3	0.67	12.0	4.0	37.0	3.1
8.0	3.9	0.1	7.0	4.0	55.0	7.9

[a] Molar concentrations $\times 10^3$. [b] $(\Delta A/\text{min}) \times 10^3$.

TABLE IV: Values of the Michaelis Constant for CO_2 at Various pH Levels.

pH	$K_{HCO_3(t)} \times 10^3$ (M)	$K_{CO_2} \times 10^4$ (M)
5.9	5.5 ± 0.2	42.0
6.5	9.6 ± 0.1	42.5
7.1	8.5 ± 0.1	14.1
7.4	4.3 ± 0.2	3.9
7.9	9.2 ± 0.1	2.9
8.2	27.1 ± 0.1	4.3
8.4	41.2 ± 0.9	4.1

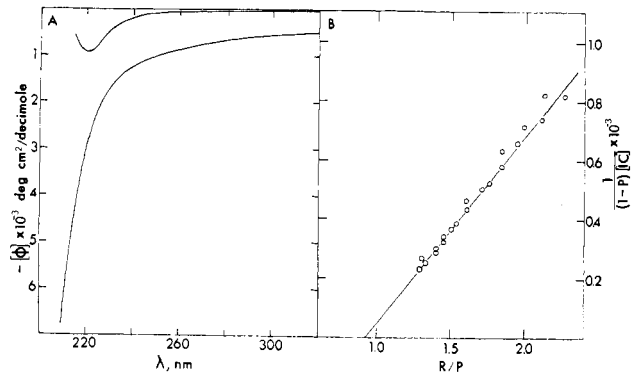

FIGURE 5: Effects of Mg^{2+} chelation on the ORD spectrum of D-isocitrate. (A) ORD spectra of D-isocitrate at pH 7.0: upper, Mg^{2+} absent; lower, Mg^{2+} present. (B) Evaluation of Mg^{2+} isocitrate chelate dissociation constant according to differential ORD analysis (Adkins and Yang, 1968). P is the ratio of apparent molar rotations at 310 nm of the partially and fully chelated forms of isocitrate corresponding to the prevailing ratio, R, of total Mg^{2+} ion to total isocitrate concentrations. The reciprocal of the slope of the line yields the dissociation constant, while the X intercept indicates the stoichiometry of the complex.

TABLE V: Effects of Magnesium Concentration on the Turnover Numbers and Michaelis Constants for the Oxidative Decarboxylation of D-Isocitrate.[a]

$MgCl_2 \times 10^3$ (M)	$(V_1/E) \times 10^{-2}$ (mol of TPNH/(min mol of IDH))	$K_{TPN^+} \times 10^5$ (M)	$K_{IC} \times 10^5$ (M)	$K_{MgIC} \times 10^5$ (M)
5	88.5 ± 1.2	2.0 ± 0.1	1.7 ± 0.1	0.873
1	91.2 ± 1.1	2.1 ± 0.1	2.8 ± 0.1	0.488
0.4	94 ± 10	2.2 ± 0.1	4.3 ± 0.2	0.335
0.2	90.9 ± 4.4	1.4 ± 0.1	4.1 ± 0.4	0.166
0.1	89.3 ± 3.0	1.6 ± 0.1	6.2 ± 0.3	0.128
0.05	82.7 ± 7.0	2.4 ± 0.5	11.5 ± 0.9	0.120

[a] All experiments were conducted in potassium phosphate buffers at pH 7.3. The ionic strength was maintained at approximately 0.13 M.

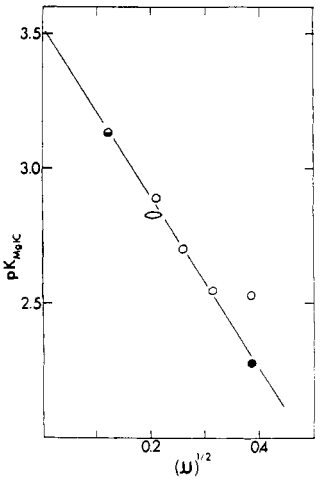

FIGURE 6: Ionic strength dependency of Mg^{2+}–isocitrate chelate dissociation constants with ionic strength. Sources of data: ○, Blair (1969); ●, Londesborough and Dalziel (1970); ◒, Duggleby and Dennis (1970); ellipse, our data from Figure 5B; the long axis of the ellipse indicates the range of ionic strength spanned by the addition of Mg^{2+} ion in the determination.

(Londesborough and Dalziel, 1970). It might be inferred from the variation of K_{IC} with Mg^{2+} ion concentration that it is actually the Mg^{2+}–isocitrate chelate which is the active substrate of this enzyme. If so, the Michaelis constant for this species should be independent of Mg^{2+} ion concentration. Some computations of K_{MgIC} were made based on reported values of the dissociation constants of the $MgHPO_4$ and Mg–isocitrate chelates, corrected for ionic strength effects (Greenwald *et al.*, 1940). The ionic strength correction applied to the isocitrate chelate dissociation constant was $pK_{MgIC} = 3.5$–3.1 $(\mu)^{1/2}$. This relation was obtained by plotting the negative decadic logarithm of dissociation constants determined by a number of workers, including ourselves, as a function of $(\mu)^{1/2}$; see Figures 5 and 6 (Duggleby and Dennis, 1970;

Blair, 1969; Londesborough and Dalziel, 1970). The pK_a for the dissociation of protons from $H_2PO_4^-$, also necessary for the computation of K_{MgIC}, was estimated to be 6.7 in the ionic strength region of the experiments under consideration (Bernhard, 1956; Alberty *et al.*, 1951). The K_{MgIC} values so calculated appear in the last column of Table V. There is some uncertainty in the values of this column, since the ionic strength dependencies of the chelate and $H_2PO_4^-$ dissociation constants are not precisely known. In addition, no correction was made for the amount of Mg^{2+} ion chelated by TPN (Colman, 1972a). As the total amount of TPN was relatively small in the kinetic experiments under consideration, the effect of Mg^{2+} ion binding by TPN on the availability of free Mg^{2+} was considered negligible. Furthermore, Mg^{2+} ion binding by TPN is presumably ionic strength dependent, and there is no information available as to how great this sensitivity is. Slight corrections, however, would not alter the observation that K_{MgIC} is not invariant with total Mg^{2+} ion concentration. The lack of constancy indicates that the postulated interaction of enzyme only with the Mg–isocitrate chelate is inadequate by itself to account for the observed behavior of the system. A mechanism invoking the existence of all the equilibria shown below is probably involved in the generation of the proposed active enzyme–substrate complex, E–Mg–isocitrate.

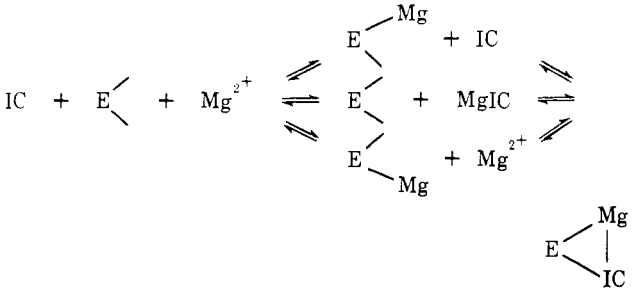

According to this scheme, the increasing values of K_{MgIC} with rising Mg^{2+} ion levels of Table V reflect the fact that at higher Mg^{2+} ion concentrations, there are fewer free sites to which the Mg–isocitrate chelate can bind, *i.e.*, the chelate must displace a Mg^{2+} ion from the enzyme before it can bind. Clearly, a knowledge of the binding of Mg^{2+} ion to the enzyme would be useful here, but at the moment, this information is unavailable for the *A. vinelandii* enzyme.

Substrate Binding. The various enzyme–substrate interactions along with the corresponding dissociation constants, as determined by ultrafiltration methods, are listed in Table VI. Representative Scatchard plots from which some of the constants of Table VI were obtained are shown in Figure 7. Isocitrate, TPN^+, and TPNH are seen to form strong complexes with IDH while 2-ketoglutarate binds much more weakly, which is in accord with the proposed random order of reactant addition and sequential order of product release.

The detection of the binding of isocitrate as monitored by optical rotation changes is illustrated in Figure 8. The saturation phenomenon observed in panel A indicates a differential molar rotation at 310 nm of about -7000 deg cm^2 dmol^{-1}, based on the molar concentration of protein. This is suggestive of the action of bound isocitrate being on the rotatory strength of a protein chromophore rather than *vice versa*, since the nearest Cotton effect for isocitrate is well below 240 nm; see Figure 5A. That this is so is observed in the circular dichroic (CD) spectra of Figure 9. Even though CD spectra in the presence of DL-isocitrate, at concentrations which would cause partial saturation, fall in between those shown in Figure 9, less than ideal signal-to-noise ratios prohibit the use of the difference in the CD spectra of bound and unbound enzyme for the measurement of binding constants. Nevertheless, there is indeed a negative CD perturbation of the the right order of magnitude, 10^4 molar ellipticity units, to account for the rotation change observed at 310 nm. From panel B of

TABLE VI: Dissociation Constants for IDH–Substrate Complexes Determined in the Presence of $MgCl_2$ at pH 7.3 in 0.05 M Potassium Phosphate Buffer.

Ligand	$MgCl_2 \times 10^3$ (M)	Reaction	$\bar{K} \times 10^5$ (M)
TPN^+	5	E–TPN^+ ⇌ E +	2.7 ± 0.6
	0[a]	TPN^+	(1.8 ± 0.9)[b]
			1.7 ± 0.2
IC	5	E–IC ⇌ E + IC	5.2 ± 0.5
	0		(2.0 ± 0.9)[b]
			5.1 ± 0.7
TPNH	5	E–TPNH ⇌ E +	4.1 ± 0.4
	0[c]	TPNH	2.6 ± 0.3
KG	10	E–KG ⇌ E + KG	118.0 ± 21
	0		74.0 ± 26
TPNH	10	E–TPNH–KG ⇌	3.0 ± 1.4
	0	E–KG + TPNH	2.1 ± 0.2
KG	10	E–TPNH–KG ⇌	27.0 ± 5.0
	0	E–TPNH + KG	45.6 ± 9.7
KG	10	E–TPN^+–KG ⇌	75.0 ± 14.6
	0	E–TPN^+ + KG	Not determined
IC	20	E–TPNH–IC ⇌	Very large
	0	E–TPNH + IC	7.3 ± 1.2
TPNH	20	E–TPNH–IC ⇌	Very large
	0	E–IC + TPNH	7.9 ± 1.3

[a] In the absence of $MgCl_2$, sufficient KCl was added to maintain the ionic strength constant. [b] Values obtained from kinetic constants of Table I and the application of relations presented in the Discussion in this paper. [c] This binding study was done at pH 8.0. In the presence of 5×10^{-3} M $MgCl_2$, at pH 8.0, $K_{TPNH} = 3.1 \pm 0.3 \times 10^{-5}$ M as determined by ultrafiltration binding studies.

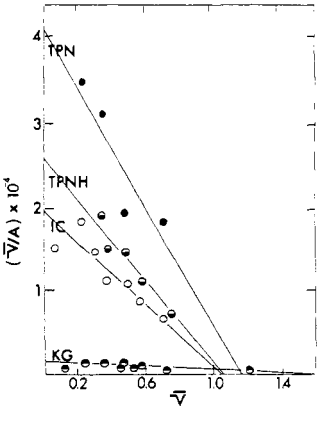

FIGURE 7: Representative Scatchard plots of ultrafiltration binding data.

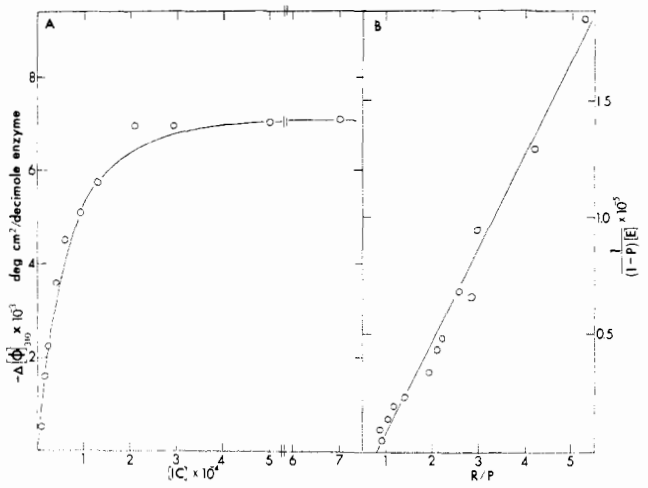

FIGURE 8: Influence of D-isocitrate on the optical rotation of isocitrate dehydrogenase at 310 nm. (A) Difference molar rotation values upon addition of DL-isocitrate to sample 5-cm cell containing 3×10^{-5} M enzyme at pH 7.0 in 10^{-2} M Mg^{2+} ion. Reference cell contained same enzyme solution, to which buffer lacking DL-isocitrate was added in volumes equal to that above. (B) Adkins–Yang plot of difference rotation data.

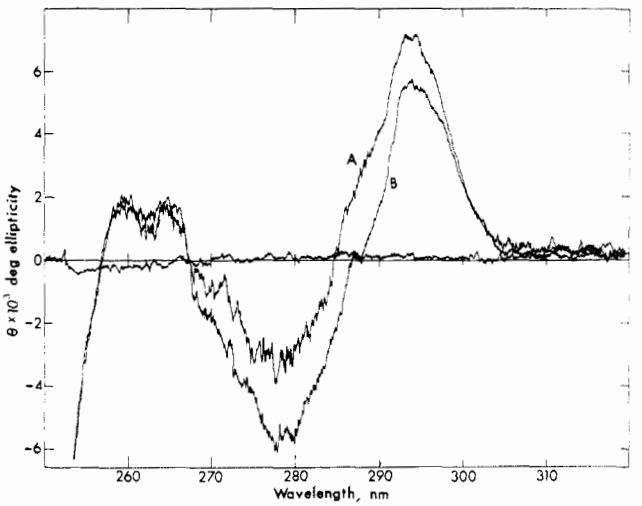

FIGURE 9: CD spectra of isocitrate dehydrogenase in free and D-isocitrate bound forms. (A) Isocitrate dehydrogenase, 2.28×10^{-5} M ($A_{279} = 1.625$), in 0.005 M $MgCl_2$–0.005 M Tris buffer, pH 8.5, in 1-cm path cell. (B) As for A, with DL-isocitrate present at a total concentration of 1.24×10^{-3} M.

Figure 8, the intercept on the abscissa indicates the formation of a 1:1 complex and the inverse of the slope yields a dissociation constant of 2.72×10^{-5} which is somewhat lower than the corresponding ultrafiltration based constant of Table VI, but is greater than the kinetically evaluated constant. The addition of TPN to the enzyme produced no detectable alterations in the CD spectrum of the enzyme in the region from 250 to 315 nm. Only limited concentrations of TPN could be tolerated because of the high absorbance of this ligand, yet at concentrations where significant binding would have been expected, no CD perturbations were produced.

Discussion

The results of the initial velocity studies in the absence of inhibitors indicate that the mechanism of the *A. vinelandii* isocitrate dehydrogenase system is indeed sequential with respect to substrate addition and product release. The existence of both the ternary complex of enzyme–isocitrate–TPN^+ and the quaternary complex of enzyme–TPNH–KG–CO_2 immediately disallows a variety of displacement mechanisms in which these complexes are not formed.

In the case of the three-substrate reductive carboxylation, the initial velocity patterns can be used to ascertain whether a compulsory order of substrate addition is required. The equation describing the initial velocity of a reaction observing an ordered sequential addition of three substrates is given by eq 6 for the addition being in the order of A first, succes-

$$\frac{1}{v} = \frac{1}{V}\left(1 + \frac{K_a}{A} + \frac{K_b}{B} + \frac{K_c}{C} + \frac{K_{ab}}{AB} + \frac{K_{bc}}{BC} + \frac{K_{abc}}{ABC}\right) \quad (6)$$

sively followed by B and C (Cleland, 1963). Notice that this equation differs from eq 5 by the omission of the term K_{ac}, *i.e.*, for an ordered reaction, K_{ac} equals zero. For saturating concentrations of either A or C, eq 6 reduces to the general equation of a two-substrate sequential addition reaction. With saturating amounts of B, however, one obtains a reciprocal rate equation formally characteristic of that of a ping-pong mechanism, *e.g.* eq 7. Therefore, if parallel double reciprocal

$$\frac{1}{v} = \frac{1}{V}\left(1 + \frac{K_a}{A} + \frac{K_b}{B}\right) \quad (7)$$

plots are obtained with respect to any of the reactants at saturating levels of the third, one could conclude that the reaction required a compulsory order of substrate addition, and that the saturating substrate involved in the parallel plots was second to add to the enzyme. Although truly parallel plots were not observed with respect to any of the reactants, Figure 1 indicates that this behavior was approached by TPNH and HCO_3^- (CO_2) at saturating levels of 2-ketoglutarate. This observation is taken to imply that, even if the reductive carboxylation reaction has no absolutely compulsory order, the principal reaction route is one in which 2-ketoglutarate adds second to the enzyme, with TPNH probably being the leading substrate rather than CO_2.

Turning our attention now to the forward reaction, if isocitrate were the initial substrate, one would expect that inhibition by TPNH would be competitive with isocitrate and noncompetitive with TPN^+. This behavior was not observed. If, on the other hand, TPN^+ were the obligatory leading substrate in the forward reaction, TPNH would be competitive with TPN and noncompetitive with isocitrate which is at least qualitatively consistent with some of the pertinent observations, *e.g.*, Figure 2B. For this mechanism with TPNH as a product inhibitor against TPN as variable substrate, the slope TPNH inhibition constant, $K_{i,TPNH}^{slope}$, should be independent of the level of isocitrate present and is identifiable as $\bar{K}_{TPNH}$, the dissociation constant for the enzyme–TPNH binary complex. Figure 3A shows that this inhibition constant is not independent of isocitrate concentration, though admittedly the variation is not sufficiently large to confidently dismiss the TPN first, isocitrate second mechanism on these grounds alone. Also, for this mechanism the $K_{i,TPNH}^{slope}$ (and $K_{i,TPNH}^{int}$) values with isocitrate as a variable substrate should

vary linearly with TPN concentration according to eq 9 and 10, respectively. It is apparent from Figure 3B that the slope

$$K_{i,TPNH}^{slope} = \bar{K}_{TPNH}\left(1 + \frac{[TPN^+]}{\bar{K}_{TPN^+}}\right) \quad (8)$$

$$K_{i,TPNH}^{int} = \bar{K}_{TPNH}\left(1 + \frac{[TPN^+]}{K_{TPN^+}}\right) \quad (9)$$

determined inhibition constant does vary linearly with TPN^+ concentration. Since our direct binding studies show that $\bar{K}_{TPN^+}$ is similar in magnitude to K_{TPN^+} similar slope and intercept effects would be expected on the basis of eq 8 and 9. Though the individual variability of the intercept determined inhibition constants does not permit any conclusions to be drawn about the TPN^+ concentration dependency for this constant, the much larger slope effects than intercept effects of Figure 2B provide a strong objection to the TPN^+ first mechanism.

We propose that the forward reaction involves a rapid equilibrium random order of addition mechanism, and we invoke the formation of a dead-end ternary complex of enzyme with isocitrate and TPNH to account for the noncompetitive nature of Figure 2B. For such a mechanism, the inhibition by TPNH should be competitive with either isocitrate or TPN^+ as the variable substrate. To achieve this response with isocitrate, the conditions of Figure 2C which ensure the availability of an ample concentration of free Mg^{2+} ion were employed. The possible functions of Mg^{2+} in this regard are discussed below. Suffice it to say here that the data of Figure 2, panels A and C, provide substantial evidence for the random order of addition reaction course.

The competitive inhibition of Figure 2A, the noncompetitive inhibition aspects of Figure 2B, and the inhibition constant behavior of Figure 3 can all be rationalized by the postulation of the aforementioned dead-end inhibitor complex. The inclusion of the dead-end complex formation in the random mechanism of substrate addition yields the prediction that TPNH inhibition against TPN should still be competitive with an inhibition constant given by

$$K_{i,TPNH}^{slope} = \bar{K}_{TPNH}\left(1 + \frac{[IC]}{K_{IC}}\frac{\bar{K}_{IC,TPNH} - \bar{K}_{TPNH}}{\bar{K}_{IC,TPNH} + \bar{K}_{TPNH}([IC]/\bar{K}_{IC})}\right) \quad (10)$$

where $\bar{K}_{IC,TPNH}$ is the equilibrium constant describing the dissociation of TPNH from the dead-end inhibitor complex. At saturating levels of isocitrate the value of inhibition constant of eq 10 asymptotically approaches the value of $\bar{K}_{IC,TPNH}$ and at extremely low isocitrate concentrations it approaches the value of $\bar{K}_{TPNH}$. Hence, such behavior as is observed in Figure 3A is consistent with the dead-end complex postulate.

It also follows from this dead-end complex postulate that the TPNH inhibition against isocitrate should be noncompetitive with the slope determined inhibition constant being given by an expression identical with the right-hand side of eq 8. The corresponding slope determined TPNH inhibition constant for the random order mechanism in the absence of dead-end complex formation is given by an expression identical with the right-hand side of eq 9. Consequently, though the pattern of inhibition constant dependency on fixed substrate concentration, as seen in Figure 3B, is of no value in differentiating between ordered and random mechanisms, it is not inconsistent with the random mechanism which invokes the enzyme–isocitrate–TPNH dead-end complex.

For the reverse reaction, the competitive nature of the TPN^+ inhibition with respect to TPNH as the variable substrate provides no new information, but is essentially consistent with the previous proposals. The observation that isocitrate behaves as a competitive inhibitor against TPNH again favors the rapid equilibrium random addition of TPN^+ and IC to the enzyme over the obligatory addition of TPN^+ as the leading substrate in the forward reaction. The apparent lack of an intercept effect, which might have been expected on the basis of the formation of the dead-end complex discussed above, could be due to the presence of high concencentrations of 2-ketoglutarate and an inferred greater stability of the enzyme–TPNH–KG ternary complex relative to the enzyme–TPNH–IC dead-end complex. The direct binding studies support this order of stabilities; see Table VI.

One can further delineate the order of substrate addition in the reverse reaction on the basis of the inhibitory behavior of 2-ketoglutarate against TPN^+ as variable substrate. By Cleland's first rule, the uncompetitive inhibition indicates that 2-ketoglutarate combines with a different form of the enzyme than does TPN^+, and that the inhibition cannot be overcome by saturation with the variable substrate (Cleland, 1963). By his second rule, these steps are not reversibly connected, otherwise a slope effect would be expected. If 2-ketoglutarate were released first by the enzyme, there would be a reversible connection between the steps involving TPN^+ and 2-ketoglutarate and a slope effect would have been observed. This strongly suggests that 2-ketoglutarate adds second in the reverse direction and, by default, that CO_2 adds third. Alternatively, in anticipation of the arguments of the next paragraph, the uncompetitive nature of the inhibition by 2-ketoglutarate can be explained by the formation of a second dead-end ternary complex, of the form enzyme–TPN^+–KG. Acting individually or in combination, these two mechanisms would result in uncompetitive inhibition with respect to TPN^+.

The noncompetitive inhibition pattern exhibited by 2-ketoglutarate against isocitrate, however, seems to require the postulation of a dead-end complex of the type just described. In the absence of dead-end complex formation, one would again expect only an intercept effect to occur; the presence of a slope effect as well implies that 2-ketoglutarate combines with the same form of the enzyme as isocitrate or with one that is separated from it by reversible steps. This is consistent with the binding of 2-ketoglutarate to the enzyme–TPN^+ complex.

Although in the forward reaction 2-ketoglutarate was an uncompetitive inhibitor of TPN^+, in the reverse reaction TPN^+ acted as a noncompetitive inhibitor of 2-ketoglutarate. Again, by Cleland's second rule, the points of addition of TPN^+ and 2-ketoglutarate are reversibly linked in the reverse direction but not in the forward direction. This is in agreement with the arguments presented thus far for the random substrate addition-ordered product release mechanism of forward reaction.

The rather unexpected small intercept effect observed with inhibition by isocitrate of 2-ketoglutarate as a variable substrate can be employed to argue for the presence of the binary complex of enzyme and ketoglutarate. The formation of this binary complex might explain the slightly nonparallel character of the reciprocal velocity *vs.* substrate concentration plots observed with saturating amounts of 2-ketoglutarate for the uninhibited reverse reaction, Figure 2. Note that these uninhibited reactions and the reverse reactions with isocitrate

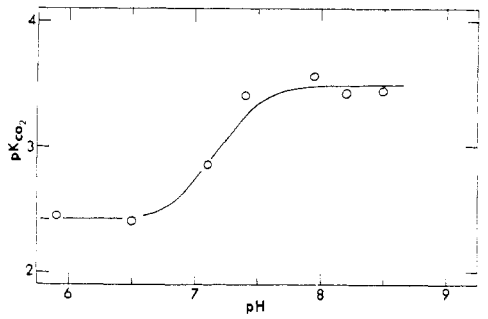

FIGURE 10: Variation of the negative logarithm of the Michaelis constant for CO_2 with pH.

as a product inhibitor of 2-ketoglutarate were carried out at relatively high concentrations of 2-ketoglutarate, in the range of 10^{-2} M, wherein one might expect that some minor, but significant, fraction of the enzyme would exist as the proposed weak binary complex. In contrast, the experiments in which 2-ketoglutarate was used as a product inhibitor were carried out at much lower 2-ketoglutarate concentrations, 10^{-4} M, which would allow for the existence of only insignificant amounts of this allegedly weak binary complex.

Granting the random addition mechanism for the forward reaction, eq 6 can be transformed to yield a rate equation (11) in which the compound kinetic constant is identified as the product of a binary complex dissociation constant and its conjugate primary Michaelis constant. In eq 11, where

$$\frac{1}{v} = \frac{1}{V}\left[1 + \frac{K_{TPN^+}}{[TPN]} + \frac{K_{IC}}{[IC]} + \frac{K_{TPN^+}K_{IC}}{[TPN^+][IC]}\right] \quad (11)$$

K_{TPN} and K_{IC} are the primary Michaelis constants, $\bar{K}_{TPN^+}$. K_{IC} is replaceable by $K_{TPN^+}\bar{K}_{IC}$. Hence, the quantities, K'_{TPN^+} and K'_{IC}, obtained as slope to intercept ratios of secondary slope plots of the uninhibited forward reaction, are identified as the dissociation constants $\bar{K}_{TPN^+}$ and $\bar{K}_{IC}$, respectively. These appear as the parenthesized values of Table VI. The similar values of the kinetically and thermodynamically determined enzyme–TPN^+ binary complex dissociation constants is gratifying. The apparent discrepancy in the values for the enzyme–isocitrate complex is not understood.

The similar magnitudes of the dissociation constants for the binary complexes of enzyme with TPN and isocitrate, Table VI, suggest that, in the cell, the extent to which the reaction proceeds through either possible forward reaction route depends on the concentration ratio of these two substrates. The ternary complex, E–TPNH–KG, was observed to be formed, Table VI, through both possible routes. However, the prior binding of TPNH enhanced the binding of 2-ketoglutarate by a factor of 4.4, whereas the prior binding of 2-ketoglutarate increased the affinity of the enzyme for TPNH by a considerably smaller factor, 1.3. This discrepancy seems to be outside experimental error, but may be explainable in terms of the dissociating influence of the enhanced ionic strength of the 2-ketoglutarate saturated medium. For obvious reasons the dissociation constants for the active ternary complex E–TPN^+–IC, releasing either TPN^+ or isocitrate, could not be directly evaluated. However, given the validity of the proposed random order addition mechanism and the fact that the primary double reciprocal plots for the uninhibited forward reaction showed common intersections on the abscissa, we can conclude that the binding of the second substrate is uninfluenced by the presence of the first.

Owing to the minor contribution of the route characterized by the binding of 2-ketoglutarate as the reverse reaction leading substrate, the Michaelis constants cannot with certainty be assigned simple identities analogous to those expressed for the forward reaction.

The existence of the dead-end complex, E–TPN^+–KG, implied by the product inhibition studies was confirmed by the binding studies summarized in Table VI. The formation of the other postulated dead-end complex, E–TPNH–IC, occurred in the absence of $MgCl_2$, but at 2×10^{-2} M $MgCl_2$ the presence of the adduct was not observed. The diminished production of this complex in the presence of high concentrations of free Mg^{2+} ion is in keeping with the formulations derived from the product inhibition data.

Although the Mg^{2+} ion stronglly influences the stability of the E–TPNH–IC dead-end complex, it appears to have little effect on the stabilities of the binary complex and the active ternary complex, E–TPNH–KG.

The role of divalent metal ion in the oxidative decarboxylation of isocitrate varies with the particular enzyme catalyzing the reaction. Duggleby and Dennis have found that the DPN-linked enzyme from pea mitochondria requires both free and metal-complexed isocitrate, but that it apparently has no requirement for free Mg^{2+} ion (Duggleby and Dennis, 1970). According to their analysis the Mg–isocitrate complex is the true substrate in the reaction and free isocitrate (or free citrate) is required as an allosteric effector. On the other hand, Cennamo *et al.*, in their work with the yeast enzyme, observed substrate inhibition by isocitrate at low Mg^{2+} ion concentrations (Cennamo *et al.*, 1967). Since isocitrate chelates Mg^{2+} ion, this finding to them indicated a requirement for free Mg^{2+} ion and nonchelated isocitrate. The reports from the laboratory of Colman on the TPN- and DPN-specific isocitrate dehydrogenases provide interesting contrasts on this theme. For example, the TPN-specific isocitrate dehydrogenase has been shown to employ the metal chelate of the tribasic form of isocitrate (Colman, 1972b), while the DPN-linked enzyme utilizes specifically the free dibasic form of the acid (Cohen and Colman, 1972). It appears from the data presented here that the *A. vinelandii* TPN-specific enzyme uses either the chelated or free forms of isocitrate, TPN^+, and TPNH, and that Mg^{2+} ion may bind to the active site of the enzyme in the absence of other substrates.

From the dependencies of the forward and reverse reaction velocities with pH, one is tempted to make tentative assignments of pK_a values for proton dissociable groups of enzyme–substrate complexes. For an enzymatically catalyzed reaction like the oxidative decarboxylation under study, this is a particularly hazardous undertaking. This is so because the two steps, oxidation and decarboxylation which taken together give the overall reaction, each involve the utilization of protons. Though protons are not represented in the overall stoichiometry, their successive production and consumption must be explicitly introduced in steady state kinetic equations which portend to describe the reaction under conditions of substrate saturation. As has been pointed out by Cleland, the effect will be to shift the usual bell-shaped V_{max} *vs.* pH plots to more acidic values if protons are consumed in some intermediate step (Cleland, 1970). In the case of isocitrate dehydrogenase, it is not possible to predict what the effect will be since it is not certain whether the same enzyme–substrate complex resulting from the oxidation of isocitrate and which yields a proton (a) is the same one which undergoes essentially simultaneous decarboxylation and proton uptake or (b) first undergoes decarboxylation and then proton uptake. These

two different mechanisms would have quite different influences on the sensitivity of V_{max} to pH and either would, depending on the magnitude of the rate constants of the internal conversion steps, affect the position on the pH axis of the function describing the relative population of the active protonated forms of the enzyme. In this context, it is of interest to note that the differences observed in the pH of the peak maximum velocities for the forward and reverse reactions can, *a priori*, just as well be attributed to differences in magnitudes of internal conversion steps as to differences in pK values of the central complexes. Some reservation must, therefore, be held with regard to accepting the validity of enzyme–substrate pK values reported for enzymes which catalyze reactions in which protons are produced and then used up (Colman and Chu, 1969).

It is significant that over the pH range covered by the kinetic experiments, the maximum velocities for both the forward and reverse reactions are sensitive functions of pH, but the Michaelis constants of the substrates TPN^+, isocitrate, TPNH, and 2-ketoglutarate are virtually unresponsive to pH changes. This finding provides additional support for the rapid-equilibrium addition of these substrates to the enzyme, since large changes in the overall rate constant or turnover number are not at all reflected in the Michaelis constants for these substrates. Thus, the overall reaction rate seems to be governed either by the oxidation of isocitrate or the decarboxylation of oxalosuccinate.

To this point in the discussion, it has been assumed that molecular CO_2 is the form of the carboxylation substrate. In support of this assumption, the general increase in velocity with time as depicted in Figure 4 is in qualitative agreement with that expected if CO_2 is the actual substrate for the reaction. The extent to which the enzymatically catalyzed carboxylation reaction velocity parallels the concentration of spontaneously generated CO_2 *via* the dehydration of HCO_3^- (CO_3^-) can be quantitatively assessed by comparing the $t_{0.5}$ and $t_{0.9}$ values of Figure 2 with the half-time and nine-tenths-time for the spontaneous dehydration reaction under like conditions. Values for $t_{0.5}$ and $t_{0.9}$ of 19 and 64 sec at pH 6.4 and of 26 and 88 sec at pH 7.2 were calculated for the conditions of the reported experiments taking into account the pH-dependent catalytic effect of HPO_4^{2-} ion on the CO_2 hydration reaction as outlined by Londesborough and Dalziel (Londesborough and Dalziel, 1968). The reasonably good agreement between the characteristic dehydration times as evaluated from enzyme reaction velocities, Figure 2 (inset), and from directly measured rate constants reported by Londesborough and Dalziel indicates that CO_2 is the strongly preferred substrate for the reductive carboxylation. These conclusions are corroborated by the character of the rate *vs.* time curves of Figure 4 for the CO_2 initiated reaction.

The initial velocity relationships of Table IV also support the assertion that CO_2, rather than HCO_3^-, is the species that adds to 2-ketoglutarate, *i.e.*, as the amount of CO_2 in the unbuffered solutions relative to that in the preequilibrated solutions increases with pH, the corresponding velocity ratio (last column) also increases.

These results are in accord with those reported by Dalziel and Londesborough for the TPN-linked isocitrate dehydrogenase from ox heart mitochondria (Dalziel and Londesborough, 1968). The same conclusion about the nature of the carboxylation substrate was suggested by Rose for the TPN-specific isocitrate dehydrogenase from pig heart (Rose, 1960). In this case the preference for CO_2 as the true substrate in the reductive carboxylation was based (a) on the increasing pH between pH 6 and 8 and (b) on the decreasing rate of reductive carboxylation over the same pH increment.

Assuming, as we have, that the rate of dissociation of CO_2 from the quaternary enzyme–substrate complex greatly exceeds its rate of incorporation into oxalosuccinate, one can employ the pH dependence of K_{CO_2} to give suggestive evidence for or against the covalent binding of CO_2 in the form of, say, a carbamate derivative. In general, either of two possible mechanisms for CO_2 addition may be utilized as illustrated in the following relations.

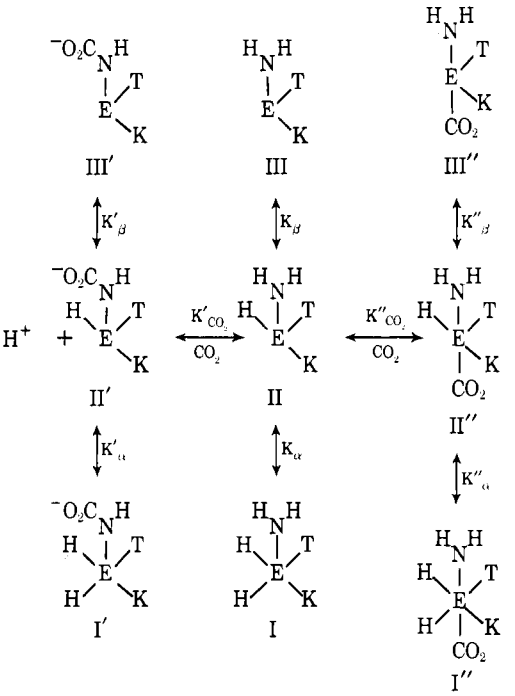

In the equilibria depicted to the left of the central column of complexes, carbamate formation is envisioned to take place, while in equilibria to the right, CO_2 is considered to be noncovalently associated with the previously formed ternary complex of the enzyme with 2-ketoglutarate (K) and TPNH (T). Note that the distinctive feature of the left-hand processes is the release of a proton upon CO_2 binding. Each row of complexes from bottom to top represents successively more basic forms of the enzyme. The quantities K'_{CO_2} and K''_{CO_2} are the CO_2 dissociation constants for the middle row of complexes and are given by eq 12 and 13.

$$K'_{CO_2} = \frac{[CO_2][II]}{[H^+][II']} \tag{12}$$

$$K''_{CO_2} = \frac{[CO_2][II]}{[II'']} \tag{13}$$

In the context of these relations and the assumed rapid equilibrium of CO_2 addition, the negative logarithm of the observed Michaelis constant can be expressed as a function of pH by eq 14 for the case of carbamate formation and by eq

$$pK_{CO_2} = pK'_{CO_2} - \log \frac{(1 + 10^{pK_a - pH} + 10^{pH - pK_\beta})}{(1 + 10^{pK_a' - pH} + 10^{pH - pK_\beta'})} + pH \tag{14}$$

$$pK_{CO_2} = pK''_{CO_2} - \log \frac{(1 + 10^{pK_a - pH} + 10^{pH - pK_\beta})}{(1 + 10^{pK_a'' - pH} + 10^{pH - pK_\beta''})} \tag{15}$$

15 for the case of noncovalent CO_2 association. Since K_{CO_2} was not measurable at pH values where the ionization of the more basic groups presumably would become important, the third terms in each of the parentheses of eq 14 and 15 will be neglected. Though this simplification probably obviates the assignment of quantitative values to the remaining parameters, the qualitative form of the pH dependency of pK_{CO_2} remains clearly different for the two suggested modes of CO_2 addition. According to the carbamate formation hypothesis the slope of a plot of pK_{CO_2} *vs.* pH should approach unity at low pH and high pH and should be greater than unity at pH values between pK_a and pK_a' for $pK_a > pK_a'$. The slope will be less than unity, but not less than zero, in the intermediate pH range if $pK_a < pK_a'$. On the other hand, if noncovalent association occurs the slope of the pK_{CO_2} *vs.* pH plot has zero slope at low and high pH and positive or negative slope in between depending on whether pK_a is greater than pK_a'' or *vice versa*. As is observed in Figure 10, the response of pK_{CO_2} to pH is such as to suggest that CO_2 adds to the enzyme without the formation of a carbamate derivative and that the process operates essentially like the Bohr effect, that is, a proton is loosened when the CO_2 adduct forms. As was indicated above, no firm statement can be made about the magnitude of the pK_a values though, provisionally, Figure 10 implies that pK_a is in the vicinity of 7.5 and pK_a' may be about 6.5.

In summary, steady state velocity studies in the absence and presence of product inhibitors support the conclusion that *A. vinelandii* isocitrate dehydrogenase catalyzes the oxidative decarboxylation of isocitrate primarily *via* the random addition of substrates and the sequential release of products in the order of molecular CO_2, 2-ketoglutarate, and TPNH. A minor route of product release involves the inversion of the departure of the last two products from the enzyme. Finally, the existence of the two dead-end complexes, enzyme–isocitrate–TPNH and enzyme–2-ketoglutarate–TPN^+, is demonstrated.

References

Adkins, B. J., and Yang, J. T. (1968), *Biochemistry 7*, 266.

Alberty, R. A., Smith, R. M., and Bock, R. M. (1951), *J. Biol. Chem. 193*, 425.

Bernhard, S. A. (1956), *J. Biol. Chem. 218*, 961.

Blair, J. M. (1969), *Eur. J. Biochem. 8*, 287.

Cennamo, C., Monteccoli, G., and Bonaretti, G. (1967), *Biochim. Biophys. Acta 132*, 232.

Chung, A. E., and Franzen, J. S. (1969), *Biochemistry 8*, 3175.

Chung, A. E., and Franzen, J. S. (1970), *Arch. Biochem. Biophys. 141*, 416.

Chung, A. E., Franzen, J. S., and Braginski, J. E. (1971), *Biochemistry 10*, 2872.

Cleland, W. W. (1963), *Biochim. Biophys. Acta 67*, 188.

Cleland, W. W. (1967), *Advan. Enzymol. 29*, 1.

Cleland, W. W. (1970), *in* The Enzymes, 3rd ed, Boyer, P. D., Ed., New York, N. Y., Academic Press, p 54.

Cohen, P. F., and Colman, R. (1972), *Biochemistry 11*, 1501.

Colman, R., and Chu, R. (1969), *Biochem. Biophys. Res. Commun. 34*, 528.

Colman, R., and Chu, R. (1970), *J. Biol. Chem. 245*, 601.

Colman, R. F. (1972a), *Anal. Biochem. 46*, 358.

Colman, R. F. (1972b), *J. Biol. Chem. 247*, 215.

Dalziel, K. (1969), *Biochem. J. 114*, 537.

Dalziel, K., and Londesborough, J. (1968), *Biochem. J. 110*, 223.

Duggleby, R., and Dennis, D. (1970), *J. Biol. Chem. 245*, 3751.

Greenwald, I., Redish, J., and Kibrick, A. C. (1940), *J. Biol. Chem. 135*, 65.

Harned, H. S., and Owen, B. B. (1958), *in* The Physical Chemistry of Electrolytic Solutions, 3rd ed, New York, N. Y., Reinhold, pp 690–694.

Langan, T. A. (1960), *Acta Chem. Scand. 14*, 936.

Londesborough, J., and Dalziel, K. (1968), *Biochem. J. 110*, 217.

Londesborough, J., and Dalziel, K. (1970), *in* Pyridine Nucleotide-Dependent Dehydrogenases, H. E. Sund, Ed., West Berlin and Heidelberg, Springer-Verlag, p 315.

Rose, Z. (1960), *J. Biol. Chem. 235*, 928.

Thompson, V., and Cleland, W. W. (1965), *Fed. Proc., Fed. Amer. Soc. Exp. Biol. 24*, 228.

Williamson, J., and Corkey, B. (1969), *Methods Enzymol. 8*, 455.